

Optical properties of femtosecond laser-treated diamond

P. Calvani · A. Bellucci · M. Girolami ·
S. Orlando · V. Valentini · A. Lettino ·
D. M. Trucchi

Received: 31 October 2013 / Accepted: 6 February 2014 / Published online: 27 February 2014
© The Author(s) 2014. This article is published with open access at Springerlink.com

Abstract A laser-induced periodic surface structure (LIPSS) has been fabricated on polycrystalline diamond by an ultrashort Ti:Sapphire pulsed laser source ($\lambda = 800$ nm, $P = 3$ mJ, 100 fs) in a high vacuum chamber ($<10^{-7}$ mbar) in order to increase diamond absorption in the visible and infrared wavelength ranges. A horizontally polarized laser beam had been focussed perpendicularly to the diamond surface and diamond target had been moved by an automated X – Y translational stage along the two directions orthogonal to the optical axis. Scanning electron microscopy of samples reveals an LIPSS with a ripple period of about 170 nm, shorter than the laser wavelength. Raman spectra of processed sample do not point out any evident sp^2 content, and diamond peak presents a right shift, indicating a compressive stress. The investigation of optical properties of fs-laser surface textured diamond is reported. Spectral photometry in the range 200/2,000 nm wavelength shows a significant increase of visible and infrared absorption (more than 80 %) compared to

untreated specimens (less than 40 %). The analysis of optical characterization data highlights a close relationship between fabricated LIPSS and absorption properties, confirming the optical effectiveness of such a treatment as a light-trapping structure for diamond: these properties, reported for the first time, open the path for new applications of CVD diamond.

1 Introduction

Since the past decades, chemically vapour deposited (CVD) diamond has harvested a growing interest due to its outstanding electronic and physical properties, such as high breakdown electric field (10^7 V/cm), high carriers' saturation velocity (1.5×10^7 cm/s), high carriers' mobility ($1,800$ cm²/Vs for electrons, $1,600$ cm²/Vs for holes) and the highest thermal conductivity among solids (22 W/cmK) [1]. CVD diamond has been successfully exploited as a material for high energy detection and dosimetry applications with remarkable performances [2–4]; nevertheless, the wide band gap of diamond (5.47 eV), makes it transparent in the visible and infrared (IR) wavelength ranges. This work aims at demonstrating the possibility of employing diamond for the fabrication of devices also for visible and IR applications by enhancing the absorption properties of the material by means of a surface laser treatment.

The laser-induced periodic surface structures (LIPSS), typically formed by single-beam femtosecond laser under certain conditions, have attracted extensive attention, including their distinguishing features, formation mechanism [5–9] and potential applications [10–12]. LIPSS have been already fabricated on diamond and morphologically investigated by other groups [13–17]. To our knowledge,

P. Calvani (✉) · A. Bellucci · M. Girolami · V. Valentini ·
D. M. Trucchi
CNR-IMIP, Institute of Inorganic Methodologies and Plasmas,
National Research Council, Via Salaria km 29.300,
Monterotondo Stazione, 00016 Rome, Italy
e-mail: paolo.calvani@imip.cnr.it

A. Bellucci
Physics Department, University of Rome Sapienza,
Piazzale Aldo Moro 2, 00185 Rome, Italy

S. Orlando
CNR-IMIP, U.O.S. PZ, Zona Industriale, 85050 Tito Scalo,
PZ, Italy

A. Lettino
CNR-IMAA, Institute of Methodologies for Environmental
Analysis, Zona Industriale, 85050 Tito Scalo, PZ, Italy

only Kononenko et al. [18] reported on optical transmission behaviour as a function of laser fluence for fs-laser-induced microstructures in bulk natural and CVD diamond. However, optical properties of fs-laser LIPSS on diamond surface have not been investigated or reported in the literature.

2 Experimental

Samples used in this work are freestanding $10 \times 10 \times 0.25 \text{ mm}^3$ thermal management grade TM180 diamond plates purchased from Element Six Ltd. The producer declares, for these specimens, a polycrystalline structure, a thermal conductivity larger than $1,800 \text{ W/mK}$, a surface roughness lower than 50 nm , a bulk resistivity higher than $10^{12} \Omega \cdot \text{cm}$ and a surface resistivity of $10^{10} \Omega \cdot \text{cm}$. The laser system employed is based on a Spectra-Physics Tsunami S—fs oscillator (pulse duration of about 100 fs , repetition rate 80 MHz , wavelength 800 nm , peak power $>0.7 \text{ W}$) pumped by a Spectra-Physics Millennia Pro 5sJS (CW, wavelength 532 nm , power 5 W). The output of the oscillator is the seed for the Spectra-Physics Spitfire Pro 100 F 1 K XP 4 W amplifier (pulse duration $<120 \text{ fs}$, repetition rate selectable in the range $1/1,000 \text{ Hz}$, wavelength 800 nm , pulse energy up to 4 mJ/pulse) pumped by a Spectra-Physics Empower 30 Q-switched DPSS (diode-pumped solid state) Nd:YLF (repetition rate $1,000 \text{ Hz}$, wavelength 527 nm , pulse energy up to 20 mJ/pulse , pulse duration minor than 100 ns). The laser beam, with an energy of 3.6 mJ/pulse ($\sim 20 \text{ J/cm}^2$ fluence), was focussed perpendicularly to the diamond plate surface by a 30 cm focal length plano-convex lens and the horizontal polarized beam had a spot size of $150 \mu\text{m}$ diameter. In these conditions, grooves are formed with an intensity higher than the diamond ablation threshold ($2 \times 10^{12} \text{ W/cm}^2$). For the treatment, the diamond target had been moved by an automated X–Y translational stage along the two directions orthogonal to the laser axis with selectable speed. The surface treatment had been performed in a high vacuum chamber ($<10^{-7} \text{ mbar}$) and samples had been treated by moving the X axis with an estimated speed of $v_x = 5 \text{ mm/s}$. After the treatment, the sample had been cleaned in a high oxidizing solution ($\text{H}_2\text{SO}_4:\text{HClO}_4:\text{HNO}_3$ in the ratio $1:1:1$) for removal of treatment residual debris.

3 Discussion

Scanning electron microscopy (SEM) image of treated diamond is shown in Fig. 1 with a 50 kX magnification factor. The formation of an LIPSS perpendicularly oriented to the polarization direction (indicated in the figure by an arrow) with a ripple period in the $170 \pm 10 \text{ nm}$ range with structures longer than $5 \mu\text{m}$ is evident.

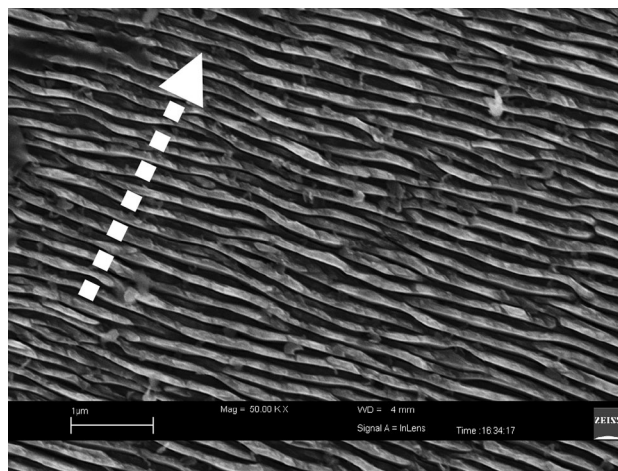


Fig. 1 SEM image of CVD diamond surface after femtosecond laser treatment. A structure with a $170 \pm 10 \text{ nm}$ periodicity has been estimated. The arrow indicates the polarization direction

The average period of induced ripples is sensibly smaller than the free-space wavelength of the laser (Ti:Sapphire at 800 nm) and this is related to the interaction between laser pulse and laser-induced plasma. The formation of this so-called high-spatial-frequency LIPSS (HSFL) has been observed for several materials and has been interpreted according to various mechanisms, such as second harmonic generation or self-organization. According to [19], we relate the ripple periodicity to the excitation of surface plasmon polaritons during the interaction between laser pulse and laser-induced plasma that generates ripples with a periodicity λ_r close to the value of $\lambda/2n$, where λ is the wavelength of the incident radiation and n the refractive index of CVD diamond, whose value at 800 nm is ~ 2.4 [20]. In good agreement with this value, average n for TM180 has been calculated from optical characterization data to be 2.4105 at 800 nm , so that the average ripple period is $\sim 167 \text{ nm}$. The lightly imperfect parallel trend observed has to be attributed to the inhomogeneous surface of the used polycrystalline diamond plate.

Micro-Raman spectroscopy has been performed in a back-scattering geometry, at room temperature, by a Dilor XY triple spectrometer, equipped with a liquid nitrogen-cooled, charge-coupled device (CCD) detector and an adapted Olympus microscope arranged in a confocal mode. The spectra had been excited with an Ar^+ laser (514.5 nm), focussed to a spot of $2 \mu\text{m}$ diameter and analyzed using a software programme to obtain, by a fitting procedure, line widths, intensities, frequencies, and components.

Raman spectra obtained for TM180 CVD diamond samples, before and after the laser treatment, are shown in Fig. 2 where sp^2 phase presence has not been noticed. In the inset, it is possible to notice a well-defined peak for

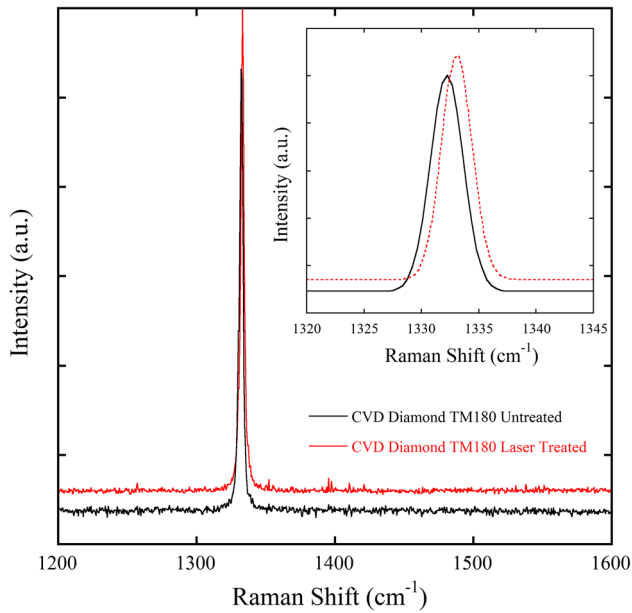


Fig. 2 Comparison of Raman spectra of CVD diamond before and after fs-laser treatment, *black* and *red* lines, respectively. Diamond peak at $1,332\text{ cm}^{-1}$ is clearly defined while sp^2 phase peak at $1,560\text{ cm}^{-1}$ is not evident, excluding graphite presence. In the inset, it is possible to notice the *right shift* of treated diamond peak, pointing out a slight compressive stress

untreated sample, marked by black line, at 1332.2 cm^{-1} , typical of diamond [21]; the treated sample, red line in the graph, shows instead a slight right shift of the peak to 1333.1 cm^{-1} , pointing out a compressive stress induced by laser irradiation. The estimated full width at half maximum (FWHM) for both samples is $3.32 \pm 0.15\text{ cm}^{-1}$, basically indicating an unperturbed order in the crystal bulk properties after the texturing process.

The characterization of the optical properties of laser-treated CVD diamond has been carried out by total transmission and reflection measurements by means of an integrating optical sphere in a spectrophotometer illuminating perpendicularly the sample with a monochromatic radiation in the wavelength range 200/2,000 nm (from ultraviolet UV to near IR). We recall that sample absorbance (A), transmittance (T) and reflectance (R) satisfy the relation $A + T + R = 1$, thus absorbance can be derived from the measurement of T and R . The spectrophotometer beam spot size is 1 cm and the sample has been mounted on a shadow mask with a 1 cm square hole, so that the whole surface is covered by photometer light. In this way, a representation of the entire diamond surface has been obtained.

In Fig. 3, the transmittance of laser-treated diamond is compared with the one of the untreated samples. It is important to notice that transmittance of TM180 polycrystalline diamond plate is lower if compared to high

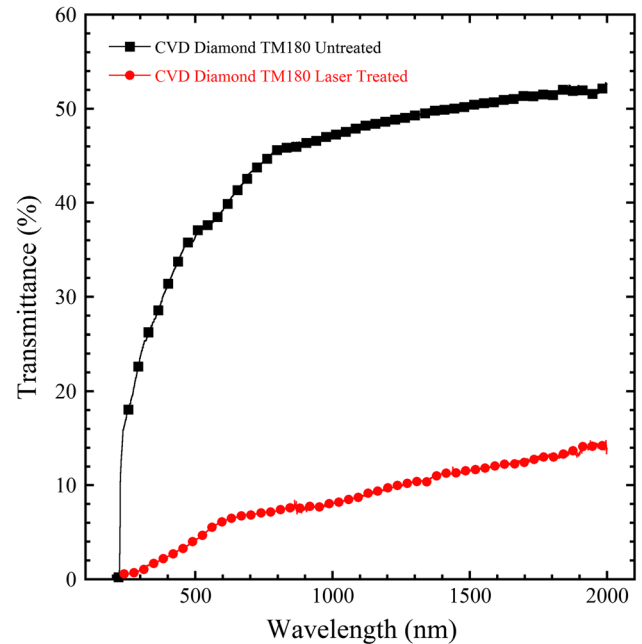


Fig. 3 Transmittance spectra of CVD diamond TM180, before and after the fs-laser treatment. The significant reduction due to laser-induced surface structure is evident

quality diamond plates reported in the literature [22, 23]. This is due to a polycrystalline structure connected to the presence of graphitic grain-boundaries, which better interact with visible-IR radiation. Laser treatment-induced defect states in diamond make T decrease more than 80 % in the visible range (i.e. from 32 to 4.5 % at 500 nm) and about 70 % in the IR (i.e. from 50.2 to 11.7 % at 1500 nm).

Absorbance data achieved for investigated polycrystalline diamond sample, before and after the laser treatment, are shown in Fig. 4. The laser treatment enhances light trapping, so that absorbance strongly increases in the entire investigated wavelength range, especially in visible and IR, up to more than 80 %. In the UV range, close to diamond band gap of 5.47 eV, corresponding to a wavelength of approximately 226 nm, absorbance reaches values of 95 %. Defining the absorbance enhancement factor k_{opt} as the ratio between treated diamond absorbance and untreated one, k_{opt} is shown in Fig. 5 as a function of wavelength: it is possible to notice that absorbance increases of a factor >2 in the entire visible range and up to more than 2.5 in the IR. Figure 5 also shows the first derivative of k_{opt} with respect to wavelength λ , $dk/d\lambda$. In first approximation, the evidence of peaks close to ripple period λ_r multiples confirms the optical effectiveness of the LIPSS as a light-trapping structure for diamond. The origin of the other peaks in the same spectrum is currently unknown and will be analyzed with further measurements.

The absorbance enhancement is mostly correlated to the decrease of diamond reflectance from about 15 to 5 % in

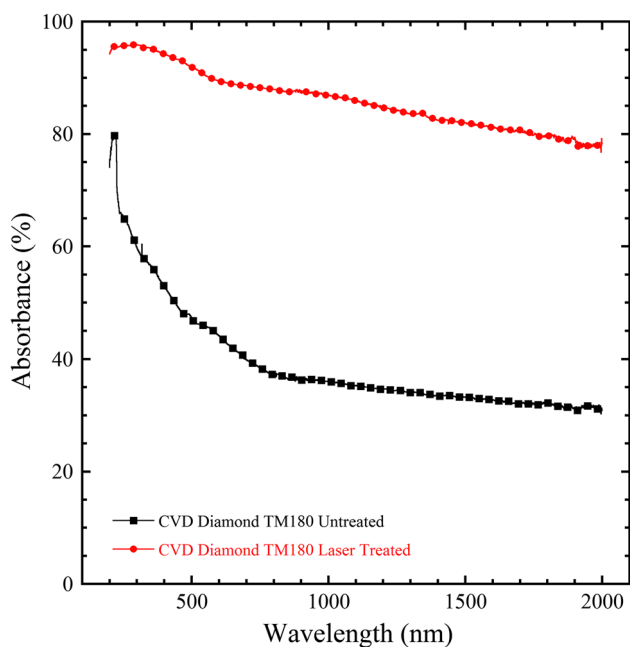


Fig. 4 Absorbance spectra of CVD diamond TM180 before and after fs-laser treatment. The light-trapping enhancement due to fs-laser treatment is revealed by absorbance increase in the entire investigated wavelength range

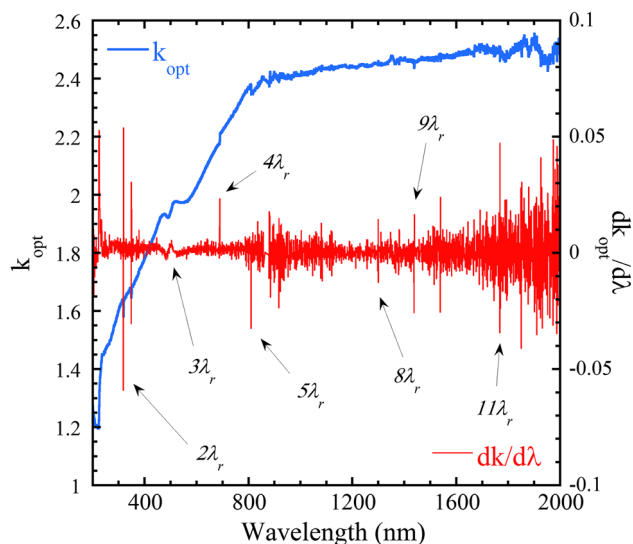


Fig. 5 Enhancement factor k_{opt} points out a strong enhancement of the absorbance in visible and infrared wavelength ranges. First derivative of k_{opt} with respect to wavelength λ highlights peaks in correspondence of ripple period λ_r multiples

all the investigated range apart from UV range, where reflectance decreases from 25 to 5 % (not shown).

The aim of this activity is the development of enhanced diamond radiation detectors, sensitized also for visible and IR spectral range. Laser treatment evidently introduces surface defect states within the diamond band gap that

could act as traps or recombination centres. The last ones are to be avoided since they do not contribute to the conduction. The step forward lies in understanding the energy position within the band gap of these defects and consequently the electric effect on the material photoconductive response. Electrical photoconductivity measurements supported by spectroscopic models [24] will be performed to investigate the efficiency of the treatment in terms of quantum yield enhancement in the visible and IR wavelength ranges.

4 Conclusion

Horizontally polarized femtosecond Ti:Sapphire pulsed laser ($\lambda = 800$ nm, $P = 3$ mJ, 100 fs) has been used to fabricate an LIPSS on polycrystalline diamond surface. The interaction between laser pulse and laser-induced plasma excites surface plasmon polaritons that generate ripples with a periodicity of $\lambda/2n$; such periodicity has been confirmed by SEM images of treated samples. The comparison of Raman spectra for processed and unprocessed samples does not point out any graphitic phase and diamond peak reveals a slight compressive stress, even if comparable FWHM for both samples indicates an unperturbed order in the crystal. We also reported for the first time the characterization of optical properties performed by spectral photometry in the range 200/2,000 nm wavelength. A significant increase of visible and infrared absorption (higher than 80 %) compared to untreated specimens (lower than 40 %) is evident. Data analysis points out the close relationship between generated LIPSS and absorption properties and confirms the optical effectiveness of the LIPSS as a light-trapping structure for diamond. Next step will be electrical photoconductivity measurements to investigate the efficiency of the LIPSS in terms of quantum yield enhancement in the visible and IR ranges.

Acknowledgments The activity was supported by the European Community FP7-Energy Project ProME³ThE²US² “Production Method of Electrical Energy by Enhanced Thermal Electron Emission by the Use of Superior Semiconductors”, Grant Agreement No. 308975, website: www.prometheus-energy.eu.

Open Access This article is distributed under the terms of the Creative Commons Attribution License which permits any use, distribution, and reproduction in any medium, provided the original author(s) and the source are credited.

References

1. R. Sussmann, J. Brandon, S. Coe, *Ind. Diam. Assoc. Am.* (1998)
2. D.M. Trucchi, P. Allegrini, P. Calvani, A. Galbiati, K. Oliver, G. Conte, *IEEE Elect. Dev. Lett.* **33**, 615 (2012)
3. D.M. Trucchi, P. Allegrini, A. Bellucci, P. Calvani, A. Galbiati, M. Girolami, *NIM A* **718**, 373 (2013)

4. A. Pietropaolo, C. Andreani, M. Rebai, L. Giacomelli, G. Gorini, E. Perelli Cippo, M. Tardocchi, A. Fazzi, G. Verona Rinati, C. Verona, M. Marinelli, E. Milani, C. D. Frost, E. M. Schooneveld, *EPL Europhys. Lett.* **92**, 68003 (2010)
5. T. Tomita, Y. Fukumori, K. Kinoshita, S. Matsuo, S. Hashimoto, *Appl. Phys. Lett.* **92**, 013104 (2008)
6. S. Sakabe, M. Hashida, S. Tokita, S. Namba, K. Okamuro, *Phys. Rev. B* **79**, 033409 (2009)
7. G. Seifert, M. Kaempfe, F. Syrowatka, C. Harnagea, D. Hesse, H. Graener, *Appl. Phys. A* **81**, 799 (2004)
8. R. Le Harzic, H. Schuck, D. Sauer, T. Anhut, I. Riemann, K. König, *Opt. Expr.* **13**, 6651 (2005)
9. E.M. Hsu, T.H.R. Crawford, C. Maunders, G.A. Botton, H.K. Haugen, *Appl. Phys. Lett.* **92**, 221112 (2008)
10. A.Y. Vorobyev, C. Guo, *Appl. Phys. Lett.* **92**, 041914 (2008)
11. A. Vorobyev, V. Makin, C. Guo, *Phys. Rev. Lett.* **102**, 234301 (2009)
12. N. Yasumaru, K. Miyazaki, J. Kiuchi, *Appl. Surf. Sci.* **254**, 2364 (2008)
13. A.M. Ozkan, A.P. Malshe, T.A. Railkar, W.D. Brown, M.D. Shirk, P.A. Molian, *Appl. Phys. Lett.* **75**, 3716 (1999)
14. Q. Wu, Y. Ma, R. Fang, Y. Liao, Q. Yu, X. Chen, K. Wang, *Appl. Phys. Lett.* **82**, 1703 (2003)
15. M. Shinoda, R.R. Gattass, E. Mazur, *J. Appl. Phys.* **105**, 053102 (2009)
16. O.H.Y. Zalloum, M. Parrish, A. Terekhov, W. Hofmeister, *Opt. Expr.* **18**, 13122 (2010)
17. S. Su, J. Li, G.C.B. Lee, K. Sugden, D. Webb, H. Ye, *Appl. Phys. Lett.* **102**, 231913 (2013)
18. T.V. Kononenko, M. Meier, M.S. Komlenok, S.M. Pimenov, V. Romano, V.P. Pashinin, V.I. Konov, *Appl. Phys. A* **90**, 645 (2007)
19. T.T.J.-Y. Derrien, T.E. TE Itina, R. Torres, T. Sarnet, M. Sentis, *J. Appl. Phys.* **114**, 083104 (2013)
20. Z. Yin, Z. Akkerman, B. Yang, F. Smith, R.E. Ted, *Diam. Relat. Mater.* **6**, 153 (1997)
21. D.M. Trucchi, E. Cappelli, G. Conte, G. Mattei, C. Gramaccioni, P. Ascarelli, *Diam. Relat. Mater.* **14**, 575 (2005)
22. W.J.P. Enkevort, E.H. Versteegen, *J. Phys. Condens. Mat.* **4**, 2361 (1992)
23. P. Dore, A. Nucara, D. Cannavò, G. De Marzi, P. Calvani, A. Marcelli, R. S. Sussmann, J. Whitehead, A. C. N. Dodge, A. J. Krehan, H. J. Peters, *Appl. Opt.* **37**, 5731 (1998)
24. M. Girolami, A. Bellucci, P. Calvani, R. Flammini, D.M. Trucchi, *Appl. Phys. Lett.* **103**, 083502 (2013)